
Prospective Study Evaluating Na¹⁸F PET/CT in Predicting Clinical Outcomes and Survival in Advanced Prostate Cancer

Andrea B. Apolo¹, Liza Lindenberg², Joanna H. Shih³, Esther Mena², Joseph W. Kim¹, Jong C. Park¹, Anna Alikhani², Yolanda Y. McKinney², Juanita Weaver^{2,4}, Baris Turkbey², Howard L. Parnes¹, Lauren V. Wood⁵, Ravi A. Madan¹, James L. Gulley¹, William L. Dahut¹, Karen A. Kurdziel², and Peter L. Choyke²

¹Genitourinary Malignancies Branch, Center for Cancer Research, National Cancer Institute, National Institutes of Health, Bethesda, Maryland; ²Molecular Imaging Program, Center for Cancer Research, National Cancer Institute, National Institutes of Health, Bethesda, Maryland; ³Biometric Research Branch, Division of Cancer Treatment and Diagnosis, National Cancer Institute, National Institutes of Health, Bethesda, Maryland; ⁴Clinical Research Directorate/Clinical Monitoring Research Program, Leidos Biomedical Research, Inc., Frederick National Laboratory for Cancer Research, Frederick, Maryland; and ⁵Vaccine Branch, Clinical Trials Team, Center for Cancer Research, National Cancer Institute, National Institutes of Health, Bethesda, Maryland

This prospective pilot study evaluated the ability of Na¹⁸F PET/CT to detect and monitor bone metastases over time and its correlation with clinical outcomes and survival in advanced prostate cancer.

Methods: Sixty prostate cancer patients, including 30 with and 30 without known bone metastases by conventional imaging, underwent Na¹⁸F PET/CT at baseline, 6 mo, and 12 mo. Positive lesions were verified on follow-up scans. Changes in SUVs and lesion number were correlated with prostate-specific antigen change, clinical impression, and overall survival. **Results:** Significant associations included the following: SUV and prostate-specific antigen percentage change at 6 mo ($P = 0.014$) and 12 mo ($P = 0.0005$); SUV maximal percentage change from baseline and clinical impression at 6 mo ($P = 0.0147$) and 6–12 mo ($P = 0.0053$); SUV change at 6 mo and overall survival ($P = 0.018$); number of lesions on Na¹⁸F PET/CT and clinical impression at baseline ($P < 0.0001$), 6 mo ($P = 0.0078$), and 12 mo ($P = 0.0029$); and number of lesions on Na¹⁸F PET/CT per patient at baseline and overall survival ($P = 0.017$). In an exploratory analysis, paired ^{99m}Tc-methylene diphosphonate bone scans (^{99m}Tc-BS) were available for 35 patients at baseline, 19 at 6 mo, and 14 at 12 mo (68 scans). Malignant lesions on Na¹⁸F PET/CT ($n = 57$) were classified on ^{99m}Tc-BS as malignant 65% of the time, indeterminate 25% of the time, and negative 10% of the time. Additionally, 69% of paired scans showed more lesions on Na¹⁸F PET/CT than on ^{99m}Tc-BS. **Conclusion:** The baseline number of malignant lesions and changes in SUV on follow-up Na¹⁸F PET/CT significantly correlate with clinical impression and overall survival. Na¹⁸F PET/CT detects more bone metastases earlier than ^{99m}Tc-BS and enhances detection of new bone disease in high-risk patients.

Key Words: prostate cancer; NaF PET/CT; sodium fluoride; bone metastases; nuclear imaging in prostate cancer

J Nucl Med 2016; 57:886–892

DOI: 10.2967/jnumed.115.166512

Prostate cancer is the most common noncutaneous malignancy in men in the United States, with an estimated 250,000 new cases and approximately 29,000 deaths annually (1). Although most patients present with localized disease and have an excellent prognosis, a subgroup of patients will develop metastases (2). Also, despite initial response to chemical or surgical castration, many patients develop resistant disease that recurs or progresses (3). Despite dramatic recent advances in the treatment of metastatic castration-resistant prostate cancer, and the approval by the U.S. Food and Drug Administration of 5 systemic therapies since 2010, prostate cancer remains the second leading cause of cancer death in men in the United States (4,5).

Approximately 90% of patients with metastatic castration-resistant prostate cancer have bone metastases (6), the primary cause of morbidity and mortality. ^{99m}Tc-methylene diphosphonate bone scanning (^{99m}Tc-BS) is currently the most widely used method for detecting bone metastasis; however, Na¹⁸F PET combined with CT has higher sensitivity and specificity.

Na¹⁸F PET/CT provides rapid (within 1 h), bone-specific uptake and blood clearance and excellent visualization of the axial skeleton. The ability of Na¹⁸F PET/CT to detect skeletal metastases has been evaluated in various types of cancer, including prostate cancer, and a series of studies has reported improved sensitivity and specificity compared with ^{99m}Tc-BS (7–13). In 2011, the Food and Drug Administration approved a new-drug application for Na¹⁸F PET/CT from the National Cancer Institute; however, its routine clinical use is not yet defined.

This pilot study assessed the ability of Na¹⁸F PET/CT to detect and monitor bone metastases over time in prostate cancer patients either on surveillance or on active therapy and correlated these data with clinical markers and survival. We hypothesized that changes in Na¹⁸F PET/CT over time, and their overall trend, would predict clinical outcomes.

MATERIALS AND METHODS

Patients

This was a prospective, 2-arm pilot study of prostate cancer patients from November 2010 to April 2013. Arm 1 accrued patients with known bone metastases on standard imaging modalities such as CT or ^{99m}Tc-BS any time before enrollment. Arm 2 accrued patients without known bone metastases but who were at high risk for metastases based

Received Sep. 4, 2015; revision accepted Dec. 15, 2015.

For correspondence or reprints contact: Andrea B. Apolo, Genitourinary Malignancies Branch, Center for Cancer Research, National Cancer Institute, National Institutes of Health, 10 Center Dr., 12N226, MSC 1906, Bethesda, MD 20892.

E-mail: andrea.apolo@nih.gov

Published online Jan. 21, 2016.

COPYRIGHT © 2016 by the Society of Nuclear Medicine and Molecular Imaging, Inc.

on a rising level of prostate-specific antigen (PSA) (30 patients per arm; $n = 60$) (Table 1). All participants underwent Na¹⁸F PET/CT at baseline, 6 mo, and 12 mo. Patients could be undergoing treatment at

any time point or be under surveillance. Patients with both castration-sensitive and castration-resistant tumors were enrolled. Patients had to have a PSA level of at least 10 ng/mL or a PSA doubling time of less

TABLE 1
Patient Demographics and Clinical Characteristics

Characteristic	Known bone metastases at enrollment	
	Negative ($n = 30$)	Positive ($n = 30$)
Age (y)		
Median	65	64.5
Range	43–79	44–79
Baseline PSA (ng/mL)		
Median	10.97	9.93
Range	0.01–190	0.1–593
Gleason score		
4	1 (3%)	0
6	4 (13%)	3 (10%)
7	7 (23%)	10 (33%)
8	8 (27%)	5 (17%)
9	9 (30%)	11 (37%)
10	0	1 (3%)
On treatment at NIH		
Yes	6 (20%)	11 (37%)
No	24 (80%)	19 (63%)
Managed at NIH multidisciplinary clinic		
Yes	10 (33%)	2 (7%)
No	20 (66%)	28 (93%)
Primary therapy		
Radical prostatectomy	14 (47%)	13 (43%)
External-beam radiation	8 (26%)	7 (23%)
Brachytherapy	2 (7%)	0
Castration status		
Sensitive	21 (70%)	13 (43%)
Resistant	9 (30%)	17 (57%)
Therapy while on study		
GnRH agonist/antagonist (leuprorelin/degarelix)	28	26
Antiandrogen (bicalutamide, nilutamide)	14	13
Ketoconazole	1	4
Enzalutamide	0	1
Abiraterone	0	1
Docetaxel, bevacizumab, lenalidomide, prednisone	0	10
Taxane	0	2
Bisphosphonate (zoledronic acid/dasatinib)	3	6
Sipuleucel-T	0	3
Vaccine study (TARP, Prostavac [Bavarian Nordic])	3	4
TRC105 (TRACON Pharmaceuticals)	1	1
Radiation	4	4

NIH = National Institutes of Health; GnRH = gonadotropin-releasing hormone; TARP, T-cell receptor γ alternate reading frame protein.

Total number of patients is 60. Data are number of patients, unless otherwise indicated.

TABLE 2

Distribution of Malignant Bone Metastases on Na¹⁸F PET/CT

Location	Scans with ≥1 lesion
Skull	19 (13%)
Spine	34 (24%)
Pelvic bones	40 (28%)
Thorax	34 (24%)
Long bones	15 (11%)
Superscan	8

than 6 mo, and either no known bone metastases on standard imaging (e.g., ^{99m}Tc-BS or CT) or any PSA level and known bone metastases on standard imaging. All patients must have received primary definitive therapy. Patients with soft-tissue-only metastases were excluded. Clinical study data included the start and discontinuation dates of all antineoplastic therapy, any concomitant medications, the PSA level at the time of each Na¹⁸F PET/CT scan, and the results of clinical ^{99m}Tc-BS and anatomic imaging such as CT or MRI. Patients receiving treatment were assessed for response using the criteria of the Prostate Cancer Working Group 2 (14); Na¹⁸F PET/CT scans did not guide clinical decisions.

This study was approved by the National Cancer Institute Institutional Review Board at the Center for Cancer Research in Bethesda, Maryland. Written informed consent was obtained from each patient who participated in the study.

Imaging Techniques

Patients were injected with 111–185 MBq (3–5 mCi) of Na¹⁸F. Two hours after injection, imaging was performed on a Gemini TF system (Philips Healthcare). ^{99m}Tc-BS and Na¹⁸F PET/CT were analyzed and reviewed separately by 3 experienced nuclear medicine physicians. Differences were resolved through consensus. Lesions on Na¹⁸F PET/CT were classified as benign, malignant, or indeterminate on the basis of their location and accompanying CT features. Lesions were considered benign if located at a joint, if characteristic of degenerative changes, or if accompanied by a history of trauma in that region. Lesions were classified as malignant if they had a characteristic osteoblastic appearance on CT. Lesions with focal radiotracer uptake but no correlative CT findings were considered indeterminate. Scan results were categorized as positive if any malignant lesion was present. Ground-glass bone lesions on CT were categorized as malignant. Na¹⁸F PET/CT scans were interpreted without knowledge of the results of other imaging modalities.

Low-dose CT transmission scans were obtained (120 kVp, 60 mAs, 0.75-s rotation time, 1.438 pitch, and 5-mm axial slice thickness) for

attenuation correction and localization. Emission PET images were obtained at 2 min per bed position with 22 slices in bed overlap. PET images were reconstructed using the Gemini TF default reconstruction algorithm (BLOB-overall survival-TF: a 3-dimensional ordered-subset iterative time-of-flight reconstruction technique using 3 iterations, 33 subsets, and 4 × 4 × 4 mm voxels). Imaging review and analysis were performed using software from MIM Software, Inc.

Data Analysis

Na¹⁸F PET/CT Classification. At 6 and 12 mo, scans were categorized as showing progressive disease if there were any new lesions, stable disease if there were no new lesions, and improved disease if there was resolution of previous lesions.

SUV. Per lesion, SUV was defined as the mean of the upper 20th percentile of pixel values (80% threshold). SUV_{max} (of all identified lesions) at baseline and maximal percentage change in SUV (of all identified lesions between 2 consecutive visits) at follow-up were used to correlate with clinical outcomes.

Statistical Analysis

The primary objective of this study was to assess the reproducibility of bone uptake of Na¹⁸F. The study required 60 patients (30 in each arm) to obtain the 95% confidence interval for the mean percentage change of ±3.7%. These results have been previously reported (15). The secondary objective of the study, as reported here, was to assess changes in Na¹⁸F over time and their ability to predict clinical outcomes.

The magnitude of per-lesion change in serial SUV measures was assessed by the critical percentage change, defined as [exp (Z_{0.975} × √2 × σ) – 1] × 100 (σ = SD due to within-lesion variability of serial SUV; Z_p = pth quantile standard normal distribution).

SUV_{max} at baseline and maximal percentage change in SUV, number of lesions, and PSA were compared with respect to clinical impression. Differences in the distribution of maximal percentage change in SUV, number of lesions, and PSA percentage change with respect to clinical outcome (progressive disease/stable disease/improved disease) were tested by the nonparametric Kruskal–Wallis rank test. The association between PSA and SUV used the Spearman rank correlation coefficients. Receiver-operating-characteristic (ROC) analysis was performed, and area under the curve was estimated to assess the feasibility of using maximal percentage change in SUV from baseline to 6 mo to evaluate the patients’ progression status (progressive disease vs. stable disease/improved disease).

The Cox proportional hazards model was used to determine the prognostic value of number of lesions and change in SUV on survival. ROC analysis evaluated the predictive value of SUV maximal percentage change on 2-y survival after the 6-mo scan. Statistical analysis used R, version 3.1.0 (16). ROC analysis with binary outcome was implemented with the R package ROCR (16), and ROC analysis of survival outcome was implemented with the R package Survival ROC.

TABLE 3

Number of Na¹⁸F PET/CT Lesions with Respect to Clinical Impression at Each Time Point

Time point	Data			P
Baseline	Arm 1, 5 (0–52)	Arm 2, 0 (0–4)		<0.0001
Clinical impression at 6 mo	Improved, 3 (0–29)	Stable, 2 (0–24)	Progressed, 14 (2–65)	0.0078
Clinical impression at 12 mo	Improved, 6 (1–29)	Stable, 1 (0–26)	Progressed, 25 (0–59)	0.0029

Total number of lesions is 60. Data are median number of lesions, followed by range in parentheses.

RESULTS

We performed 170 Na¹⁸F PET/CT scans on 60 prostate cancer patients (60 at baseline, 58 at 6 mo, and 52 at 12 mo), 84% of which demonstrated bone lesions. At baseline Na¹⁸F PET/CT, 239 lesions were evaluable. The number of lesions per patient ranged from 0 to 52 at baseline, 0 to 65 at 6 mo, and 0 to 59 at 12 mo. Eight patients had superscans, defined as showing more than 50 lesions. In this case, one lesion was selected per anatomic site (5 lesions per superscan per patient). Table 2 shows the distribution of malignant bone metastases on Na¹⁸F PET/CT.

SUV

We recorded the SUV for each lesion. Maximal percentage change in SUV from baseline to the 6-mo and 6- to 12-mo scans correlated with clinical impression (mean maximal percentage change, 141% [$P = 0.0147$]; mean maximal percentage change, 157% [$P = 0.0053$], respectively).

The ROC analysis of maximal percentage change in SUV with respect to progressive disease at 6 mo yielded a 0.84 area under the curve (95% confidence interval, 0.62–0.98). The threshold of SUV maximal percentage change was 57.1%, with sensitivity of 75% (6/8), specificity of 82.8% (24/29), positive predictive value of 54.5% (6/11), and negative predictive value of 92.3 (24/26). There was a significant increase in SUV between 6 and 12 mo in patients who progressed at 12 mo ($P = 0.005$).

Number of Lesions

The median and range for number of lesions with respect to clinical impression at each scan are shown in Table 3. The distributions of the number of lesions with respect to clinical impression were significantly different at 6 and 12 mo ($P < 0.01$).

PSA

At baseline, patients with metastatic lesions had significantly higher PSA levels than those without metastases ($P = 0.016$). The correlation between change in PSA and SUV maximal percentage change at 6 mo ($R^2 = 0.39$; $P = 0.014$) and 12 mo ($R^2 = 0.58$; $P = 0.0005$) was also significant. Examples of Na¹⁸F PET/CT change with PSA are seen in Figure 1.

Survival

Median follow-up was 35 mo (range, 17–45 mo), during which 18 patients died. The Cox proportional hazards model estimated the effects of covariates on overall survival. The number of lesions at baseline Na¹⁸F PET/CT correlated significantly with overall survival ($P = 0.017$). SUV_{max} at baseline was not a significant predictor, but maximal percentage change at 6 mo correlated with survival ($P = 0.018$; hazard ratio, 1.23 for 50% maximal percentage change). ROC analysis 2 y after the 6-mo Na¹⁸F PET/CT scan had an area under the curve of 0.88 (95% confidence interval, 0.76–0.97). At the threshold of 50.4% change in SUV, sensitivity and specificity were 73% (11/15) and 78% (18/23), respectively. Eleven of 16 patients whose change in SUV exceeded the threshold died.

Longitudinal Observation

Arm 1, the metastatic group, had the largest number of deaths (14 vs. 4 in arm 2); it also had 2 patients without definite bone lesions on any of the 3 Na¹⁸F PET/CT scans. This calls into question the original classification based on prior ^{99m}Tc-BS. The metastatic group also had 11 patients with increasing numbers of lesions at follow-up; 6 of these patients died. There were more deaths in patients with fluctuations in lesion number at follow-up than in those with stable lesion number at follow-up.

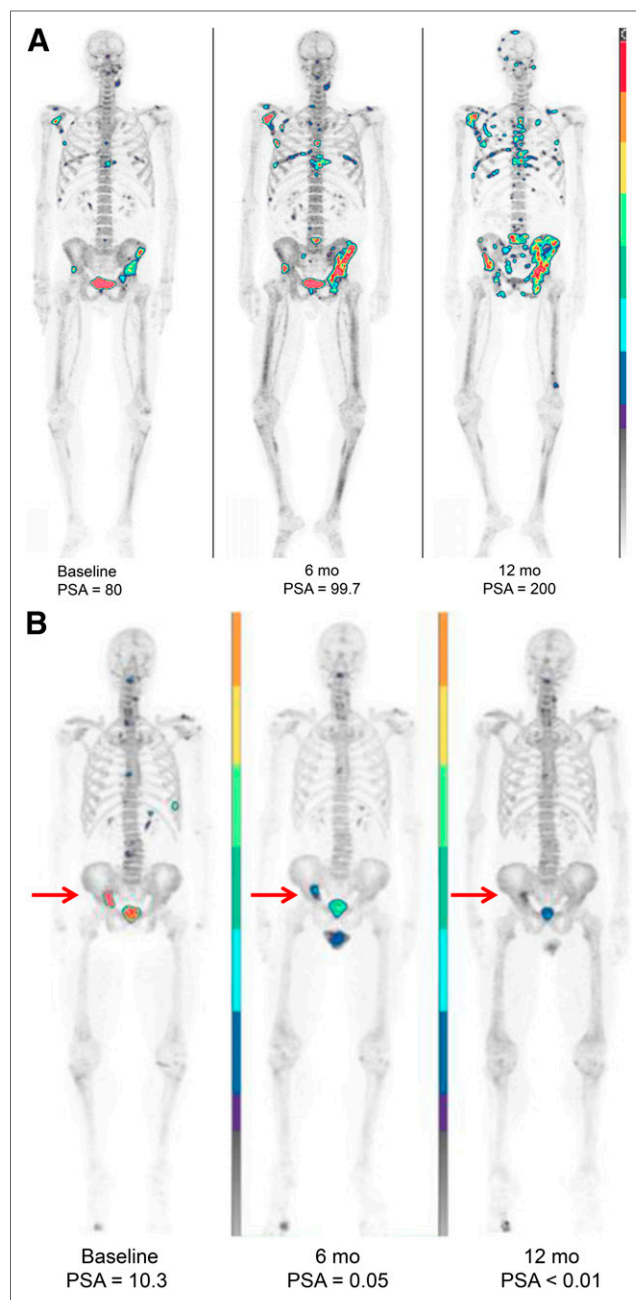


FIGURE 1. (A) Progressive disease on Na¹⁸F PET/CT in 67-y-old man with postdocetaxel metastatic castration-resistant prostate cancer whose PSA level increased on treatment with abiraterone acetate (6 mo) and cabazitaxel (12 mo). Sequential Na¹⁸F PET/CT scans detected multiple new skeletal lesions. Image intensities were equally adjusted. (B) Improved disease on Na¹⁸F PET/CT in 66-y-old man with metastatic castration-resistant prostate cancer who had PSA response to docetaxel chemotherapy. Sequential Na¹⁸F PET/CT scans showed significant decrease in uptake in right pelvic skeletal lesion. Image intensities were equally adjusted.

In Arm 2, the nonmetastatic group, 14 of 30 patients (baseline PSA, 0.06–190) had bone metastasis on baseline Na¹⁸F PET/CT (range, 1–7; average, 3); 7 had no change in lesion number on the 2 follow-up scans; 3 died. The other half of this arm ($n = 16$) had no bone metastasis on baseline Na¹⁸F PET/CT and did not develop bone

lesions on follow-up. This arm also had more patients ($n = 22$) with no change in lesion number on follow-up scans.

Ground-Glass Lesions on CT

Focal Na^{18}F uptake in bone lesions without an apparent CT correlate was noted in 26 of 60 patients. These 26 patients had an average of 17 lesions identified by Na^{18}F PET/CT, of which approximately 4 lesions per patient (107 total) revealed a subtle CT ground-glass appearance on closer scrutiny. In 18 patients, the ground-glass lesions changed to dense lesions in 35 of 107 lesions (33%) and from dense to ground-glass in 6 of 107 lesions (5%) (in patients on hormonal therapy). In 8 patients, the majority of lesions (62%) remained unchanged. Patients whose ground-glass lesions became denser were 9.4 times more likely to show disease progression at 12 mo than patients without ground-glass lesions ($P = 0.0152$), potentially indicating an early opportunity for therapeutic intervention.

Na^{18}F PET/CT Versus $^{99\text{m}}\text{Tc}$ -BS

A patient-based analysis of 68 paired Na^{18}F PET/CT and $^{99\text{m}}\text{Tc}$ -BS images in 37 patients taken at baseline ($n = 35$), the 6-mo follow-up ($n = 19$), and the 12-mo follow-up ($n = 14$) (Fig. 2; Table 4) compared detection of bone metastases. The results demonstrated 66% concordance (45/68) between Na^{18}F PET/CT and $^{99\text{m}}\text{Tc}$ -BS in terms of final impression (37 positive, 3 indeterminate, and 5 negative) (Table 4). Na^{18}F PET/CT detected more lesions in 47 of 68 paired scans (69%) (Fig. 2) (mean, 4 more lesions per patient). Figure 3 shows an example of lesions seen on Na^{18}F PET/CT versus $^{99\text{m}}\text{Tc}$ -BS.

Fibrous Dysplasia

Fibrous dysplasia, an incidental radiologic finding, is scarlike tissue that develops in place of normal bone. It is generally considered a pediatric condition and is usually asymptomatic (17,18). Monostotic fibrous dysplasia is more prevalent in craniofacial bones, where it is typically diagnosed radiographically by its

characteristic radiolucency, resembling ground glass or heterogeneous sclerosis. We detected 8 incidental cases (13%) of fibrous dysplasia in the Na^{18}F PET/CT scans among the 60 patients on study, limited to the ethmoid (2/8), nasal (5/8), and sphenoid (1/8) bones of the skull (Fig. 4).

DISCUSSION

Prostate cancer progression is characterized by a variety of disease states, including clinically localized disease, rising-PSA noncastrate, rising-PSA castration-resistant, clinically metastatic noncastrate, and clinically metastatic castration-resistant (19). Bone metastases are a frequent manifestation, yet there is no accurate quantitative method for imaging prostate cancer metastases in bone (20). Na^{18}F PET/CT has been studied mostly in the clinically metastatic castration-resistant state, and its role in earlier disease states has not been established. Several studies have evaluated the ability of Na^{18}F PET/CT to detect bone metastases compared with other nuclear and radiologic modalities, with highly favorable results for Na^{18}F PET/CT (7–13,21,22). Na^{18}F PET/CT demonstrated high reproducibility in a prospective study of dual baseline scans in patients with prostate cancer and multiple myeloma (15), supporting its clinical value in oncology practice. Still, many clinicians are reluctant to embrace Na^{18}F PET/CT as it is unclear whether it is overly sensitive and thus does not accurately represent disease status.

Here, we longitudinally evaluated Na^{18}F PET/CT in prostate cancer patients and compared results to clinical outcomes. In both arms of the study, most patients had stable Na^{18}F PET/CT results over the course of a year. Patients with known bone metastasis who had increases in lesion number had shorter survival. Na^{18}F PET/CT detected more bone lesions than $^{99\text{m}}\text{Tc}$ -BS in 69% of patients (Fig. 2). The number of lesions detected at baseline Na^{18}F PET/CT significantly correlated with overall survival, and the distribution of lesions correlated with clinical impression (therapy received, PSA, $^{99\text{m}}\text{Tc}$ -BS, and CT or MRI results) at each time point (baseline, 6 mo, and 12 mo) (Table 3).

Several quantitative measures on Na^{18}F PET/CT appeared to correlate with clinical parameters. For instance, percentage change in SUV at follow-up was associated with both clinical impression and 2-y overall survival. Patients with a larger increase in SUV at the 6-mo scan tended to have shorter survival. A multicenter Na^{18}F PET/CT study (NCT01516866) is under way in patients with metastatic castration-resistant prostate cancer receiving either microtubule-directed chemotherapy or androgen-directed therapy. Patients are scanned before therapy is initiated and during treatment. This study will aid in determining the Na^{18}F PET/CT SUV change that constitutes treatment response or failure.

Our longitudinal data analysis revealed that malignant lesions on Na^{18}F PET/CT remained positive at 6 and 12 mo unless the patient received effective therapy (Fig. 1). Although confounding factors such as uptake in benign bone lesions (i.e., fibrous dysplasia), urinary excretion potentially

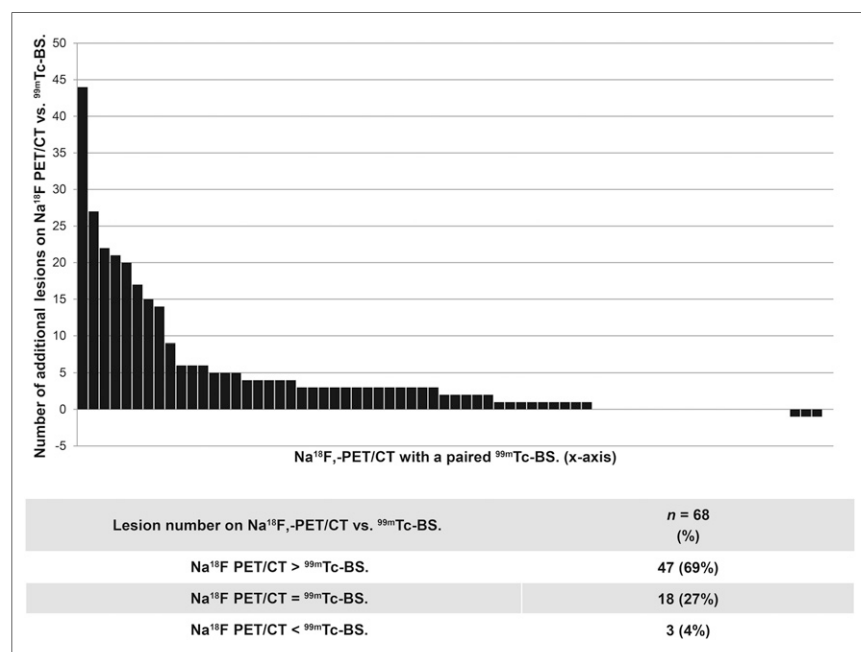


FIGURE 2. Number of lesions on Na^{18}F PET/CT vs. $^{99\text{m}}\text{Tc}$ -BS.

TABLE 4

Detection of Lesions by Na¹⁸F PET/CT and ^{99m}Tc-BS in Patient-Based Analysis

Na ¹⁸ F PET/CT	^{99m} Tc-BS		
	Positive	Indeterminate	Negative
Positive	37	14	6
Indeterminate	0	3	0
Negative	1	2	5

Total number of scans is 68.

impeding visualization of the pelvis, and tumor flare (23) after therapy remain problematic, this study demonstrated the feasibility of monitoring the response of metastatic bone lesions simply by monitoring lesion count on Na¹⁸F PET/CT imaging. To our knowledge, this is the first report of follow-up Na¹⁸F scans of prostate cancer patients over a 1-y period correlated with survival.

In our study, the concordance of lesion number between Na¹⁸F PET/CT and ^{99m}Tc-BS was 66% (44/68), with Na¹⁸F PET/CT showing higher specificity in detecting early metastatic disease, consistent with previous studies (7–13,21). Six patients with negative and 14 with indeterminate ^{99m}Tc-BS scans evidenced malignant bone disease on corresponding Na¹⁸F PET/CT (Table 4). Among the 30 men enrolled in the nonmetastatic arm, 14 (40%) were found to have malignant bone lesions on baseline Na¹⁸F PET/CT (range, 1–7; average, 3), confirming prior studies suggesting that Na¹⁸F PET/CT is more sensitive than ^{99m}Tc-BS in detecting early metastatic disease (7–13,21). In the evolving and complex therapeutic arena of prostate cancer, earlier detection of metastatic disease would be particularly helpful when counseling men on the role of definitive local therapy, which is generally not recommended in the setting of clinically demonstrable metastatic disease. Clinicians are concerned

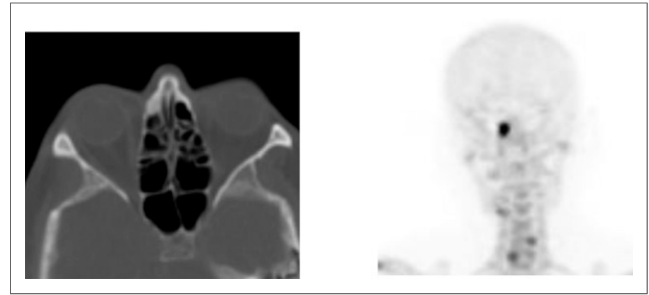


FIGURE 4. Incidental finding of fibrous dysplasia on Na¹⁸F PET/CT. Right nasal bone appears characteristically opaque and expansile. Left image is axial CT scan of skull in bone window; right image is frontal maximum-intensity-projection Na¹⁸F PET/CT scan of skull.

that detecting progressive disease on Na¹⁸F PET/CT may lead to premature discontinuation of an effective therapy, as all current therapies for prostate cancer were Food and Drug Administration–approved using ^{99m}Tc-BS as the standard metric.

Several prior studies have noted that focal Na¹⁸F uptake is more sensitive than CT scans, which often show normal findings at the hot spot on PET (9). On closer inspection, areas with focal uptake may demonstrate subtle ground-glass opacity (24) on CT, a phenomenon seen in 26 (43%) of our patients. We noted distinctly different SUVs in ground-glass lesions versus dense sclerotic lesions at baseline evaluation. Our analysis did not reveal an association between ground-glass lesions, their SUVs, and clinical outcome but did find that patients with ground-glass lesions became more sclerotic and had a higher risk of clinical progression than patients with no ground-glass lesions. The ability to identify bone metastases with functional Na¹⁸F PET/CT imaging before anatomic CT findings may help to change management strategies.

Falsely increased ¹⁸F-FDG activity in benign bone lesions such as fibrous dysplasia has often been reported. In this study, Na¹⁸F PET/CT detected 8 cases of fibrous dysplasia, all located in the skull, suggesting that it is more common than suspected and that Na¹⁸F PET/CT may be more sensitive for fibrous dysplasia than conventional ^{99m}Tc-BS. The ability of CT to demonstrate the characteristic appearance of fibrous dysplasia in bone was extremely helpful in properly diagnosing these cases as benign.

This pilot study was limited by a heterogeneous patient population that included patients with castration-resistant and hormone-responsive prostate cancer. A study involving a larger patient population may validate our conclusions. A further limitation was the difficulty of obtaining histopathologic confirmation of metastatic bone lesions. Finally, the study was not powered to compare Na¹⁸F PET/CT with ^{99m}Tc-BS. Many patients had paired Na¹⁸F PET/CT and ^{99m}Tc-BS studies at the 3 time points. Therefore, the number of lesions and the patient-based classification on both scans were compared only preliminarily.

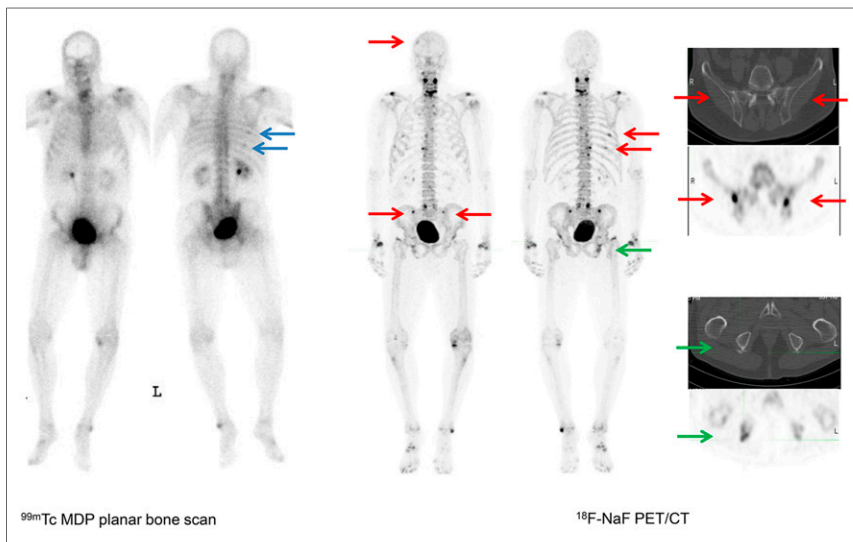


FIGURE 3. ^{99m}Tc-BS and Na¹⁸F PET/CT in 74-y-old man with high-risk prostate cancer. ^{99m}Tc-BS shows right rib lesions categorized as indeterminate (blue arrows). Na¹⁸F PET/CT confirms lesions as malignant and shows additional malignant lesions in skull, ribs, and pelvis (red arrows). Other uptake (green arrow) is consistent with degenerative change. MDP = methylene diphosphonate.

CONCLUSION

Na¹⁸F PET/CT detects more bone metastases than ^{99m}Tc-BS and detects them earlier in the disease course. Over the 12 mo of this trial, the number of lesions at baseline Na¹⁸F PET/CT and their SUV change were associated with clinical impression and overall survival. Patients with fewer bone lesions tended to have a better prognosis. Greater change in SUV at 6 and 12 mo correlated with greater change in PSA. A larger percentage increase in SUV was associated with clinical impression of progressive disease and shorter survival.

In this study, patients who had an SUV change of at least 50.4% had a significantly higher risk of death. We also found that subtle ground-glass opacities on CT, coincident with positive Na¹⁸F uptake, are likely to represent early metastatic lesions. Additionally, the unexpectedly high rate of incidental detection of fibrous dysplasia suggests that this benign condition is more prevalent than previously suspected and is detected more frequently with Na¹⁸F PET/CT. Our analysis demonstrates that Na¹⁸F PET/CT may be a useful tool in the diagnosis, prognosis, and follow-up of prostate cancer patients at high risk for bone metastasis. This study provides preliminary data to accurately power larger studies evaluating response to therapy. Further studies are warranted to assess whether castration sensitivity and type of therapy affect the ability of Na¹⁸F PET/CT to accurately identify response to treatment.

DISCLOSURE

The costs of publication of this article were defrayed in part by the payment of page charges. Therefore, and solely to indicate this fact, this article is hereby marked "advertisement" in accordance with 18 USC section 1734. This project has been funded in whole or in part with federal funds from the National Cancer Institute, National Institutes of Health, under contract HHSN261200800001E. The content of this publication does not necessarily reflect the views or policies of the Department of Health and Human Services, nor does mention of trade names, commercial products, or organizations imply endorsement by the U.S. government. No other potential conflict of interest relevant to this article was reported.

ACKNOWLEDGMENT

We thank Bonnie L. Casey for editorial assistance in the production of this article.

REFERENCES

1. Siegel RL, Miller KD, Jemal A. Cancer statistics, 2015. *CA Cancer J Clin*. 2015;65:5–29.
2. Tannock IF, de Wit R, Berry WR, et al. Docetaxel plus prednisone or mitoxantrone plus prednisone for advanced prostate cancer. *N Engl J Med*. 2004;351:1502–1512.

3. Osborn JR, Chodak GW. Natural history of early localized prostate cancer [letter]. *JAMA*. 2004;292:1549.
4. Siegel R, Naishadham D, Jemal A. Cancer statistics, 2012. *CA Cancer J Clin*. 2012;62:10–29.
5. Siegel R, Ma J, Zou Z, Jemal A. Cancer statistics, 2014. *CA Cancer J Clin*. 2014;64:9–29.
6. Bubendorf L, Schopfer A, Wagner U, et al. Metastatic patterns of prostate cancer: an autopsy study of 1,589 patients. *Hum Pathol*. 2000;31:578–583.
7. Even-Sapir E, Metser U, Mishani E, Lievshitz G, Lerman H, Leibovitch I. The detection of bone metastases in patients with high-risk prostate cancer: ^{99m}Tc-MDP planar bone scintigraphy, single- and multi-field-of-view SPECT, ¹⁸F-fluoride PET, and ¹⁸F-fluoride PET/CT. *J Nucl Med*. 2006;47:287–297.
8. Schirrmester H, Guhlmann A, Elsner K, et al. Sensitivity in detecting osseous lesions depends on anatomic localization: planar bone scintigraphy versus ¹⁸F PET. *J Nucl Med*. 1999;40:1623–1629.
9. Schirrmester H, Guhlmann A, Kotzerke J, et al. Early detection and accurate description of extent of metastatic bone disease in breast cancer with fluoride ion and positron emission tomography. *J Clin Oncol*. 1999;17:2381–2389.
10. Grant FD, Fahey FH, Packard AB, Davis RT, Alavi A, Treves ST. Skeletal PET with ¹⁸F-fluoride: applying new technology to an old tracer. *J Nucl Med*. 2008;49:68–78.
11. Langsteiger W, Heinisch M, Fogelman I. The role of fluorodeoxyglucose, ¹⁸F-dihydroxyphenylalanine, ¹⁸F-choline, and ¹⁸F-fluoride in bone imaging with emphasis on prostate and breast. *Semin Nucl Med*. 2006;36:73–92.
12. Lee SJ, Lee WW, Kim SE. Bone positron emission tomography with or without CT is more accurate than bone scan for detection of bone metastasis. *Korean J Radiol*. 2013;14:510–519.
13. Hetzel M, Arslanemir C, Konig HH, et al. F-18 NaF PET for detection of bone metastases in lung cancer: accuracy, cost-effectiveness, and impact on patient management. *J Bone Miner Res*. 2003;18:2206–2214.
14. Scher HI, Halabi S, Tannock I, et al. Design and end points of clinical trials for patients with progressive prostate cancer and castrate levels of testosterone: recommendations of the Prostate Cancer Clinical Trials Working Group. *J Clin Oncol*. 2008;26:1148–1159.
15. Kurdziel KA, Shih JH, Apolo AB, et al. The kinetics and reproducibility of ¹⁸F-sodium fluoride for oncology using current PET camera technology. *J Nucl Med*. 2012;53:1175–1184.
16. The R project for statistical computing. The R Foundation website. <http://www.R-project.org/>. Accessed March 10, 2016.
17. Choi YY, Kim JY, Yang SO. PET/CT in benign and malignant musculoskeletal tumors and tumor-like conditions. *Semin Musculoskelet Radiol*. 2014;18:133–148.
18. Su MG, Tian R, Fan QP, et al. Recognition of fibrous dysplasia of bone mimicking skeletal metastasis on ¹⁸F-FDG PET/CT imaging. *Skeletal Radiol*. 2011;40:295–302.
19. Scher HI, Morris MJ, Kelly WK, Schwartz LH, Heller G. Prostate cancer clinical trial end points: "RECIST"ing a step backwards. *Clin Cancer Res*. 2005;11:5223–5232.
20. Apolo AB, Pandit-Taskar N, Morris MJ. Novel tracers and their development for the imaging of metastatic prostate cancer. *J Nucl Med*. 2008;49:2031–2041.
21. Chakraborty D, Bhattacharya A, Mete UK, Mittal BR. Comparison of ¹⁸F-fluoride PET/CT and ^{99m}Tc-MDP bone scan in the detection of skeletal metastases in urinary bladder carcinoma. *Clin Nucl Med*. 2013;38:616–621.
22. Hillner BE, Siegel BA, Hanna L, Duan F, Shields AF, Coleman RE. Impact of ¹⁸F-fluoride PET in patients with known prostate cancer: initial results from the National Oncologic PET Registry. *J Nucl Med*. 2014;55:574–581.
23. Wade AA, Scott JA, Kuter I, Fischman AJ. Flare response in ¹⁸F-fluoride ion PET bone scanning. *AJR*. 2006;186:1783–1786.
24. Vargas HA, Wassberg C, Fox JJ, et al. Bone metastases in castration-resistant prostate cancer: associations between morphologic CT patterns, glycolytic activity, and androgen receptor expression on PET and overall survival. *Radiology*. 2014;271:220–229.